Soft Matter

PAPER

View Article Online
View Journal | View Issue

Cite this: *Soft Matter*, 2018, **14**, 3783

Compositional ripening of particle-stabilized drops in a three-liquid system

Javier Otero,[a] Steven Meeker[b] and Paul S. Clegg *[a]

Received 21st December 2017,
Accepted 16th April 2018

DOI: 10.1039/c7sm02502e

rsc.li/soft-matter-journal

We present experimental studies of two aqueous drops, stabilized by colloidal silica, which are placed close to each other in a bath of toluene, ethanol and surplus colloidal silica. If one of the drops is enriched in ethanol while the other is pure water then we observe the spontaneous formation of small droplets at the surface of the water drop closest to its neighbour. These droplets are then observed to form all along the path to the ethanol enriched drop until they make a complete bridge. We relate this behaviour to the diffusion pathways on the underlying three-fluid phase diagram. We argue that the phenomena is a version of compositional ripening where the transfer of the dispersed phase leads to the spontaneous formation of droplets in the continuous phase. We show that, while the large drops are particle-stabilized, the spontaneously formed droplets are not. Instead the presence of surplus particles leads to the droplets gelling as an elastic bridge. The phenomenology at long times and at low particle concentrations becomes increasingly surprising.

1 Introduction

Much current attention is focused on functional droplets able to perform a wide range of roles, from reactors in microfluidic devices[1] to containers for biological cells while they are analysed.[2] The ability to dynamically control the size and composition of droplets mean that they also find application in, for example, electricity generation (microfluidic Kelvin device[3]), as dynamic lenses[4] or as sensors.[5,6] Particle-stabilized droplets have characteristics which could enhance functionality in some application areas;[7,8] they often have enhanced stability while, at the same time, allowing transport processes to occur through the interstitial space between particles. Provided that the particles exhibit partial wettability with the two liquids and their size is above ≈ 3 nm then they will usually become irreversibly attached to the droplet interface. When interfaces are densely coated with hard-sphere particles they acquire elastic properties, with moduli proportional to the underlying surface tension.[9] The mechanical properties are further modified by particle–particle attractions. Related emulsion based systems are being used to create protocells that communicate.[10]

In spite of the interstices, the particle-stabilized interfaces in Pickering emulsions can suppress Ostwald ripening, however, they appear not to suppress compositional ripening.[11–13] Ostwald and compositional ripening modify the evolution of an emulsion due to chemical potential differences between droplets which drive the movement of one or more components of the dispersed phase. This transfer between droplets is induced either by droplet size differences (Laplace pressure) or droplet composition differences (compositional ripening), respectively.

The exchange of material between drops is an important high-level form of functionality.[14] To study this phenomena it is useful to have an experimental system in which material is transferred in significant quantities. This can be achieved using partially miscible liquids: ternary mixtures composed of an oil, an alcohol and water often have a standard and relatively simple phase diagram. Without the alcohol, the oil and water are typically immiscible. Added alcohol improves miscibility leading to a binodal line which separates an alcohol-rich single-fluid phase from a two-phase region. Here, we are interested in a system comprised of toluene, ethanol and water, especially its behaviour as it attempts to reach compositional equilibrium. For this particular ternary system, an ethanol concentration above ≈ 60 vol% always yields a single-phase system.[15]

Even for a single particle-stabilized drop, the behaviour in a ternary liquid system can be quite unexpected. For example, if a water drop is injected into a toluene bath containing a small proportion of ethanol and interfacially active particles, it can sprout a tube which grows upwards.[16] This curious phenomena is driven by the partitioning of ethanol into the water drop, which then migrates towards the top of the drop due to its lower density. The enhanced ethanol concentration at the top of the drop softens the particle-coated interface directing the growth. The elasticity of the particle-coated interface is crucial for supporting the weight of the tube: fresh particles from the bath are adsorbed onto exposed interface during growth. Recent studies have probed the interaction between the sprouting tube and a pendant drop placed in its path.[17] The behaviour depends on

[a] *School of Physics and Astronomy, University of Edinburgh, Peter Guthrie Tait Road, Edinburgh EH9 3FD, UK. E-mail: paul.clegg@ed.ac.uk*
[b] *CNRS, Solvay, LOF, UMR 5258, Université de Bordeaux, F-33600 Pessac, France*

bath composition and drop size, as expected, but remarkably also on the time when both drops are injected. If both drops are created at similar times, then the growing drop will try to avoid meeting the pendant drop. This reflects the fact that the pendant drop has had some time to absorb ethanol from the surrounding bath while the sessile drop has been growing. Because of the ethanol depleted layer around the pendant drop, the growing tube steers towards richer ethanol zones, away from the depleted layer. However, if the pendant drop is only injected as the growing tube approaches, then there is no time for the ethanol to become depleted: the tube approaches the drop. In place of direct contact, a "bridge" forms which appears dense and dark. It was suggested by one of us that the bridge was primarily comprised of particles from the continuous phase.[17]

The observed bridge formation, which is the functionality we focus on here, is driven by the transfer of one or more components between the growing drop and the pendant drop. Such a transfer may well induce subsidiary phenomena. In a three-liquid system, components crossing the liquid–liquid interface will potentially lead to Marangoni flows and spontaneous emulsification (one variant of which is known as the Ouzo effect). The Marangoni flows are due to a gradient in surface tension and can lead to movement at the interface of the drops.[18] In the growing drop system, the varying concentration of ethanol at different heights will create such a gradient.

Spontaneous emulsification is the creation of droplets when two immiscible liquids are brought into contact without external energy being supplied.[19] Diffusion and stranding is one of the mechanisms through which this can occur.[20] It is based on the idea that local supersaturation regions produced by diffusion can lead to the creation of emulsion droplets. For example, ethanol moving from the bath into the drop can leave oil molecules stranded in the water phase, and *vice versa*. A "diffusion path theory",[21] which has been experimentally verified, can predict the behaviour of systems at the early stages, predicting if and in which phase the emulsification will take place. It is based on the idea that this phenomena happens only if the diffusion pathways connecting the phase compositions cross the binodal line. Spontaneous emulsification has importance for a variety of application areas, such as enhanced oil recovery, the production of nanoparticles and the creation of food-grade emulsions.[22–24]

Diffusion and stranding is observed in the aniseed beverage, Ouzo, which is prepared by adding water to a mixture of ethanol and a flavour oil.[25] As the ethanol partitions into the water it takes oil molecules with it rapidly leading to the supersaturation of the aqueous phase. Nucleation and growth of oil droplets follows; this phenomena and associated self assembly are currently the subject of intense research.[26–28] The late stage coarsening of the oil droplets is driven by Ostwald ripening which might be expected to lead to macroscopic phase separation. The 'Ouzo effect' occurs in a narrow region in between the binodal and spinodal lines in which metastability is possible. This effect has also been reported in multi-component drops as ethanol evaporates, pushing the composition into the Ouzo zone.[29]

In this contribution we investigate the self-assembled bridges which are observed between drops of differing composition. We find that formation is due to the water, which diffuses between the drops driven by the composition gradient. This flow destabilizes the bath phase leading to droplet formation. For clarity, we will use the term "drops" for the injected aqueous domains ($\approx$5 μL) and "droplets" ($\approx$0.5 pL) for those which form spontaneously. Our results are primarily in the form of microscopy images (including with fluorescence or Raman spectra) accompanied by analysis and explanation. While we have tried to keep the system as simple as possible, the range of phenomena observed during the later stages of our experiments is rich and diverse.

2 Methods

Typical experiments were carried out by first filling a 15.6 mL quartz sample vial or, alternatively, 1 mm path length optical cuvette (Starna Scientific) with a chosen bath composition. Next, a distilled water drop was injected and, immediately after and at a short distance, a 50/50 vol% water/ethanol drop was also injected. For macroscopic studies, drops $\approx$30 μL were injected using a Hamilton gas-tight #1750 syringe and a Kruss steel needle of 1.8 mm diameter. For microscopic studies, drops $\approx$5 μL were injected using a Hamilton Microliter #702 syringe and a Hamilton steel needle of 0.72 mm diameter. The time evolution was then recorded using a camera (Kruss EasyDrop) and/or a microscope. Most microscopy was carried out using a Nikon Eclipse E800 microscope with a ×4 objective. Other objectives have also been used to make more detailed studies. A Zeiss LSM700 confocal microscope has been used for fluorescence studies. This included the addition of fluorescein dye (Fluka Fluorescein Reag. Ph. Eur., free acid) at 0.02 wt% to the pure water drop or when fluorescent silica particles were added at 0.02 vol% to allow tracking of the particle coverage of drops. Time series were performed using bright field and fluorescence channels simultaneously. A Raman spectrometer (Horiba Jobin-Yvon LabRam HR800) with a λ = 532 nm laser was used to study the composition of the injected drops in a range of 200–4000 cm^{-1} over time. The experimental setup included a ×10 objective, a confocal hole diameter of 1000 μm, slit width of 100 μm, grating of 600 lines per mm and exposure time of 3 seconds with 3 accumulations. The area of the ethanol and water peaks was converted to compositions using a calibration curve previously obtained under the same experimental conditions. Strain sweep measurements were performed with an Anton Paar rheometer (MCR 301), with a stainless steel cone-plate geometry where the cone diameter was 50 mm, its angle 1° and the gap between them 0.1 mm. The bath has been prepared using toluene (Sigma-Aldrich, $\geq$99.7%), ethanol (Sigma-Aldrich, $\geq$99.8%) and fumed silica particles (HDK H30) with a cluster size $\approx$100 nm, which were a gift from Wacker-Chemie (Burghausen). The usual bath composition was (in volume): 90% toluene, 10% ethanol and 0.2% silica. Other compositions have also been studied, for example, varying the silica concentration to try to discern its importance and role. The particles were dispersed using an ultrasound probe (Sonics Vibracell VCX500) for a total time of 2 minutes, using 20 seconds on/off with an amplitude of 20%. Additional silica nanoparticles (radius 14 nm) were synthesised

via the Stöber method[30] and fluorescently labeled with fluorescein isothiocyanate (FITC) dye (isomer I, Sigma Aldrich) as described by Imhof *et al.*[31]

3 Results and discussion

3.1 Bridges: macroscopic view

Fig. 1(a), (c) and (e) shows two drops shortly after being injected, one of them 100% distilled water and the other 50/50 vol% water/ethanol. The pure water drop was dyed with Nile Blue A; the amount of dye observed to leave the drop was small (with any surplus dye being found at the air–liquid interface). Crucially, a kind of "bridge" can be seen developing over a period of minutes between the drops, extending from the pure water drop towards the mixed drop, Fig. 1(b) and (d). By contrast, when two (or more) injected drops have identical compositions, each of them seems to behave independently, ignoring neighbouring drops. For example, they experience a small volume expansion if the bath contains a low ethanol concentration (*e.g.*, 10%); at higher ethanol concentrations tube sprouting is observed. This is consistent with the reported diagram.[16]

Evidently, the "bridge" formation is induced by a composition difference between the drops. More experiments using different amounts of ethanol in the pair of water drops (such as 0–20% ethanol for the low concentration, or 20–50% ethanol for the high concentration) have been carried out; the same bridge formation phenomenon is observed. As the composition gradient between the two drops becomes steeper, the bridge formation time shortens. We find that the completed bridge is somewhat elastic, however, it does fracture if the drops are forced apart, Fig. 1(e)–(h). Following bridge breaking, the formation of a new bridge on the displaced drop can be seen, whereas the old bridge thins as time passes.

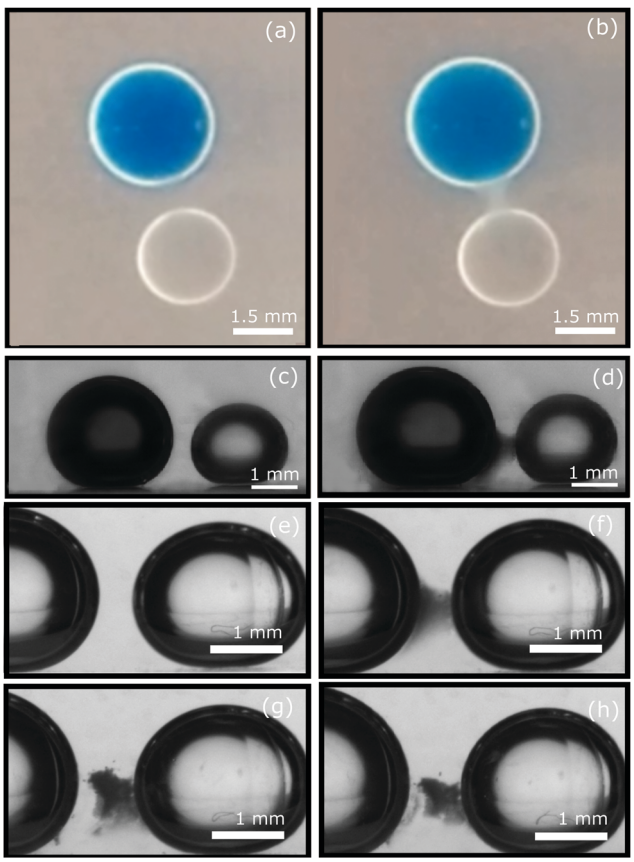

Fig. 1 (a–d) Two drops in a bath of standard composition (see Methods). The pure water drop is dyed with Nile Blue A (blue, black), the other drop is 50/50 vol% water/ethanol. (a and c) The drops soon after being injected; (b and d) 10 minutes later, a cloudy-looking connection has developed between them. (e–h) Left, pure water drop, right, 50/50 vol% water/ethanol drop with standard bath composition. (e) Immediately after injection; (f) 12 minutes later; (g) immediately after the bridge is broken; (h) 12 minutes later. The fracture of the old bridge, new bridge formation as well as thinning of the old bridge can all be observed.

3.2 Bridges: microscopic view

By confining the drops in a thin cuvette it becomes possible to observe what is happening between the drops at a microscopic scale. Using this configuration, Fig. 2(a) and (b) displays a pair of frames showing the development over time in the middle of the bridge. The standard experimental compositions and procedure (see Methods) have been followed. Clearly, the bridge is comprised of droplets of diameter $\approx$10 μm which grow slightly over a period of hours. The droplets move only slowly ($\sim$100 μm/24 hours) without being jammed into contact, which together with the bridge fracturing shown in Fig. 1(g), suggests that they might be held in place by a sparse network of nanoparticles.

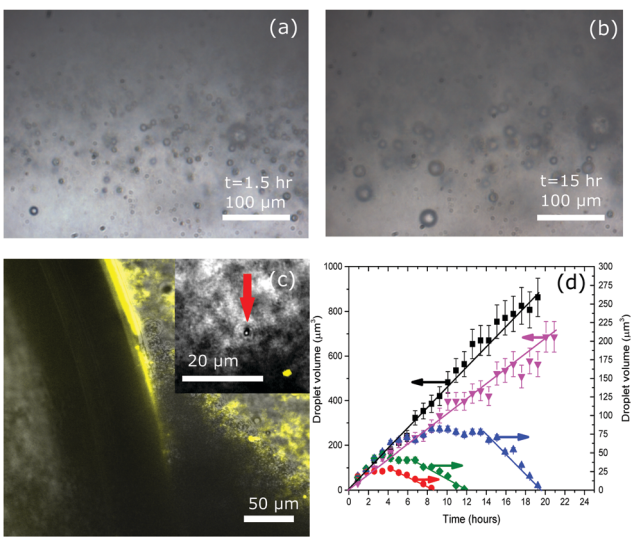

Fig. 2 (a and b) Bright-field microscopy images showing in detail what is happening in the middle of the bridge using a ×40 objective at two times. (c) Overlay confocal microscopy image of the fluorescence and transmission channels showing the interface of the pure water drop. Standard compositions and procedure were used, with the addition of a small proportion (0.02 vol%) of fluorescent silica. Coverage of the pure drop can be observed by the bright yellow lines, whereas the small droplets that form the bridge do not seem to exhibit any fluorescence. Inset: One of these droplets, indicated by a red arrow, in the middle of the bridge. (d) Volume of five spontaneously formed droplets *versus* time. Two of them are ever-increasing (left axis), whereas the others experience a decrease at about 5 hours until they redissolve. Error bars represent the standard deviation for 3 measurements. Lines are a visual guide.

Employing confocal microscopy and modifying our protocol by doping the fumed silica with a small quantity of fluorescent silica, we have studied the coverage of the liquid–liquid interfaces by such particles. Surprisingly, Fig. 2(c), we find that, whereas the injected drops are covered with silica almost immediately, the small droplets formed spontaneously appear to have no particle coverage at all. Fig. 2(d) shows the results of quantitative studies of droplet volume over time. All droplets appear spontaneously and increase in volume to make an ensemble of different sizes. Then the smaller droplets shrink until they redissolve in the bath whereas the larger droplets are shown to undergo a linear increase in volume over a period of hours. Given that the droplets are in the range 2–20 μm and that the liquid-phases exhibit some mutual miscibility, this could be Ostwald ripening; although, compositional effects due to slow changes in the bath composition are also possible.

Our bridge is made of a gelled collection of small droplets; to reveal the formation mechanism we begin by looking at how the whole structure forms. The modified (1 mm height cuvette) experimental setup has been used together with standard sample compositions (see Methods). As a representative example of these measurements, Fig. 3(a)–(d) displays a series of unprocessed frames showing the development of the bridge over time. The experimental geometry is shown inset to Fig. 3(e).

The growth behaviour was quantified by measuring the time needed for the bridge to extend to half the drops' separation as a function of separation distance. From the photomicrographs using the software Fiji[32] we found the half-way point between the drops on gray-scale images, averaged the gray intensity values over a vertical line to reduce noise and recorded the time at which a sharp decrease in intensity, corresponding to the bridge, occurs. The distance between drops *versus* these times have been fitted to a simple diffusion model (Fig. 3(e), red line), which yields a diffusion coefficient of $D = (1.18 \pm 0.14) \times 10^{-5}$ cm^2 s^{-1}, *i.e.* a value a little lower (factor of 5) than that expected for the diffusion of small molecules in these kinds of liquids.[33] While the diffusion of water may be driving the bridge growth between the drops, the phase separation in the bath may be making the process slower than expected.

We know from our fluorescence observations, Fig. 2(c), supported by observations of Ostwald ripening, Fig. 2(d), that the particles do not become trapped on the interfaces of these droplets. Additionally, the static droplets are not necessarily in contact with each other, Fig. 2(a) and (b). Clearly we need to know what the particles are doing. To this end we have studied the effect of the concentration of fumed silica particles on bridge formation, ranging from 0.0 to 0.2 vol%:

• In the absence of particles, Fig. 3(f), droplets form but they are highly mobile. The motion takes the form of transient waves which are seen between the injected drops. These intermittent and short-lived (usually less than 20 seconds) collective waves of droplets seem to travel in the same direction as in bridging experiments, *i.e.* from the pure water drop towards the mixed one. In a period of 12.5 minutes at least three distinct temporary waves were observed.

• Between 0.05 and 0.10 vol% silica, the bridge forms and extends over ~1/4–1/2 of the distance between the drops, Fig. 3(g) and (h). This partial bridge remains stable.

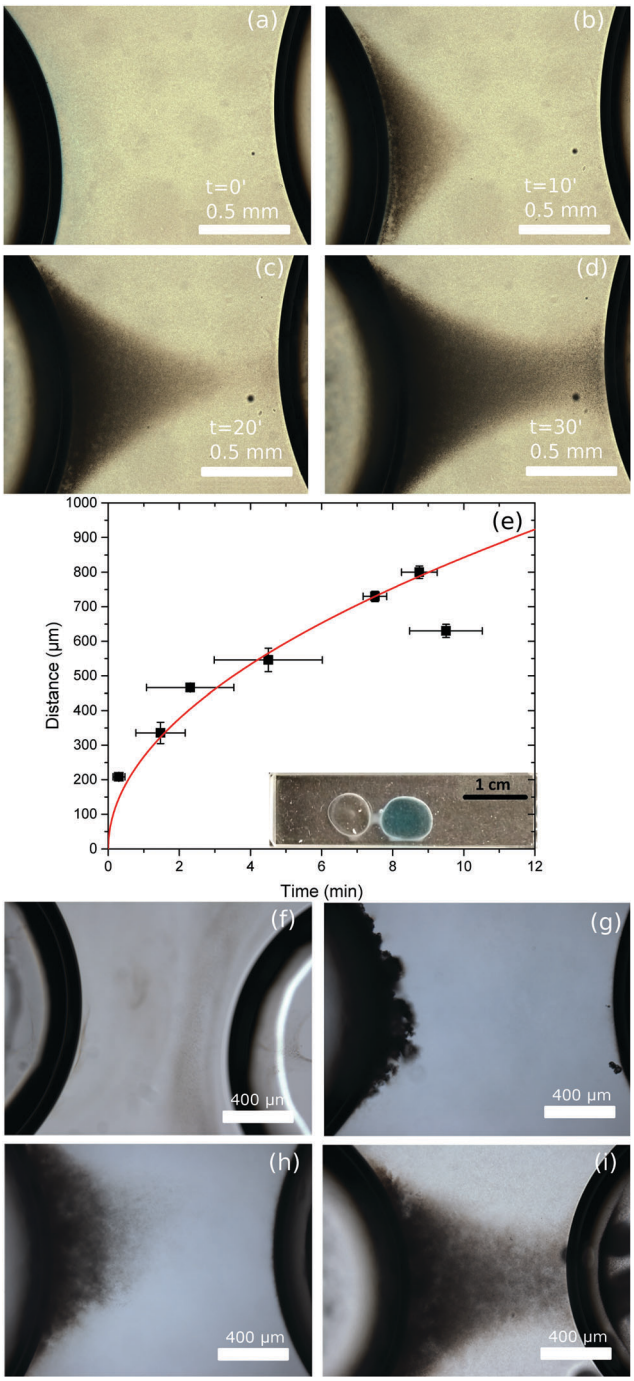

Fig. 3 (a–d) Selected frames showing a pure water drop on the left and the bridge growing towards the mixed drop on the right. (e) Time for the bridge to reach half the distance between the drops *versus* their separation distance. Red line indicates the best fit line of the function $x = \sqrt{Dt}$, where x is the distance, D the diffusion coefficient and t the time. $D = (1.18 \pm 0.14) \times 10^{-5}$ cm^2 s^{-1}. Inset shows the experimental setup used for these measurements. (f–i) Effect of varying silica particle concentration in otherwise standard bath compositions. As vol%, (f) is 0, (g) is 0.05, (h) is 0.10 and (i) is 0.15. Frames captured 10 minutes after injection, except (f), which shows a transient wave formed by droplets that only lasts around 20 seconds.

• At 0.15 vol% silica, a bridge crossing the whole divide is formed, although it is considerably less populated by spontaneous

droplets than for the standard bath composition with 0.20 vol% silica, Fig. 3(i).

This behaviour suggests that the fumed silica particles are responsible for holding the droplets in place by modifying the surrounding medium. This is presumably due to the formation of a sparse network which prevents droplet motion. We have performed a strain sweep at 1 Hz for our standard bath composition with and without silica particles, as depicted in Fig. 4(a). We observe that the storage modulus (G') dominates the loss modulus (G'') when the particles are present for strains up to 10%, indicating a weak gel-like material, whereas the loss modulus dominates, as for a liquid, if there are no particles.

In ref. 17 one of us suggested that the bridge, which was observed between the growing droplet and the newly created pendant droplet, was primarily formed from particles. Our experiments presented here demonstrate otherwise. Initially the bath phase has a composition indicated by the point where the red line meets the toluene/ethanol axis, Fig. 4(b) and (c). As water enters the bath, the composition follows the red line. Once the bath composition crosses the binodal line phase separation begins. If the bath phase remains in the region between the binodal and spinodal (the 'Ouzo' region) the phase separation remains on the level of droplets. For experiments, Section 3.3, where there is a larger composition change then macroscopic phase separation can begin. The mixed drop composition starts out at the mid-point on the water/ethanol axis, Fig. 4(b) and (d). Once the drop is within the bath, the compositions of the phases on either side of the interface have to adjust themselves, by diffusion, to become two compositions joined by a tie line. This process for the drop is indicated by the cyan line, Fig. 4(d).

A sketch of the bridge formation mechanism is shown in Fig. 4(e). Underlying this mechanism is the diffusion of water from the pure water drop to the mixed drop. The diffusion of water from a dyed (fluorescein) pure water drop, as shown in Fig. 5(a) and (b), can be seen *via* bright yellow droplets around the edges of the "bridge", whereas at the centre the amount of droplets scattering light obscure it. A further role of the water diffusing between droplets is that it destabilizes the dispersed silica particles. These partially hydrophobic particles can be dispersed reasonably successfully in a bath of toluene with ethanol. The droplet formation process, described above, will remove some ethanol from the continuous phase into the water/ethanol droplets. These changes in the bath composition may be responsible for destabilizing the dispersed particles in the space between the drops.

Thus far this is a variant of compositional ripening, which relies on the ethanol concentration in the mixed droplet remaining roughly constant. This has been probed using Raman spectroscopy to determine the water and ethanol concentration in the drops, shown in Fig. 5(c). The change in ethanol in the mixed drop is about 5% which plateaus for long time experiments as indicated in Fig. 6(e). The concentrations were obtained at the center of each injected drop. Time zero in the graph refers to the start of the Raman measurement. This occurs ~2 minutes after the injection of the drops. The legend refers to the drop being measured either as pure or mixed, referring to its initial state before injection (100% distilled water or 50/50 vol% ethanol/water), followed by the measured component (either ethanol or water).

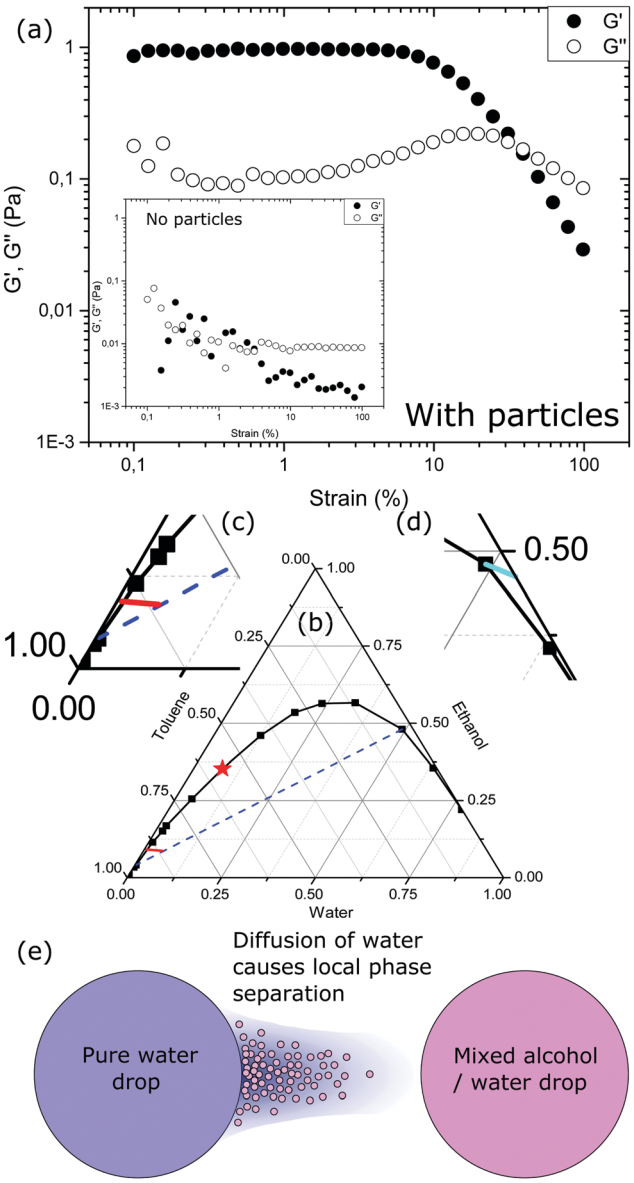

Fig. 4 (a) Strain sweep performed at 1 Hz for our standard bath composition. Inset: Strain sweep for the same bath composition with no particles. (b) Ternary phase diagram for the toluene, ethanol, water system by weight. The black line is the binodal, the red star is the critical point and the blue dashed line is a tie line. Experimental points were taken from ref. 15. (c) The bath (typically 90% toluene, 10% ethanol) moves along the red line as water diffuses in. Local phase separation occurs into a continuous phase and a droplet phase joined by a tie line. (d) The surface of the mixed drop (typically 50% water, 50% ethanol) moves along the cyan line as it comes into equilibrium with the surrounding bath. The ethanol concentration scarcely changes. (e) A cartoon of the droplet formation process. For clarity the particles on the drop interfaces and in the bath phase are not shown.

For our standard composition, careful examination reveals a further level of detail. First, at short times and over small distances

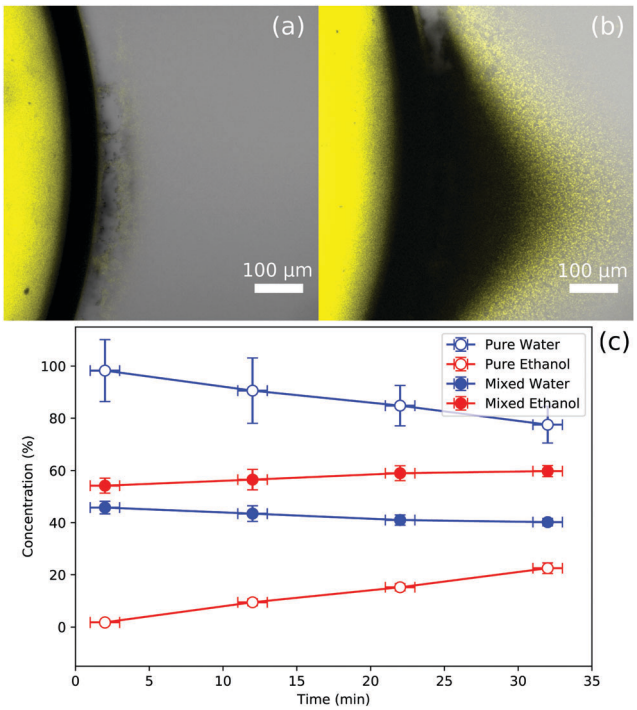

Fig. 5 (a) and (b) are composite images of the bright and fluorescent channel for a pure water-dyed drop, shortly after injection and 5 minutes later respectively. Dyed water, in the form of tiny yellow droplets, can be seen flowing from the pure drop (showed in the image) towards a mixed drop to its right. Frame (c) represents the composition of the initially pure (hollow) and initially 50/50% ethanol/water mixed (filled) drops at their center for short times (30 minutes) determined with a Raman spectrometer. Error bars indicate repeatability error.

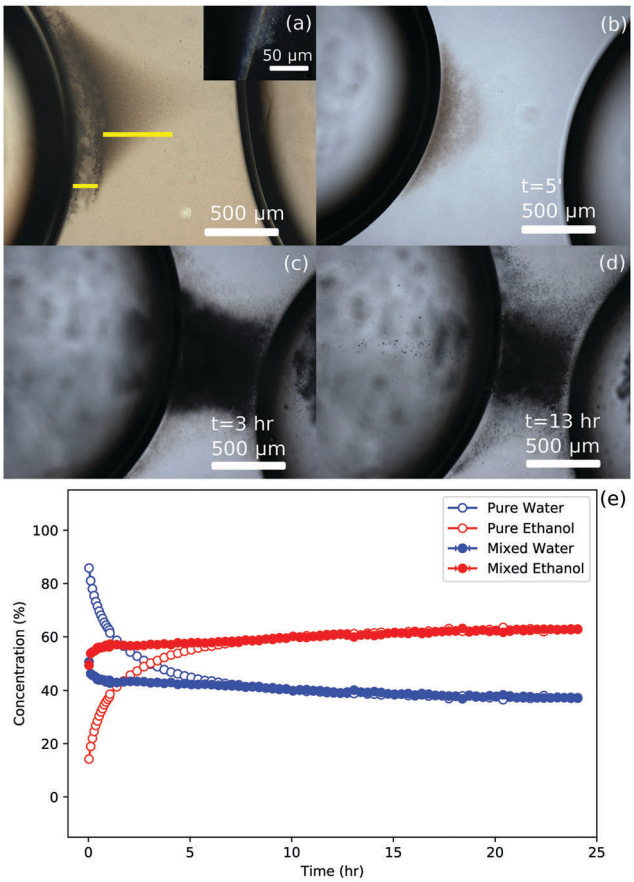

Fig. 6 (a) Showing large-scale phase separation close to the drop and droplet formation further away. Inset: A ×40 phase contrast micrograph showing in detail the droplets formed close to the water drop interface. (b–d) Bridge formation over long times. Frame (b) shows the initial stage; (c) shortly after injection droplets are observed inside the mixed drop (right); (d) finally, droplets are also observed within the water drop (left) and disappear from the mixed one. Graph (e) represents the drops' composition evolution for long time experiments (24 hours) obtained with the Raman spectrometer. In the legend, pure refers to a 100% water drop (hollow), and mixed to a 50/50 vol% (filled) water/ethanol drop.

(≈20% of drops' separation), a phase separation process takes place, Fig. 6(a). A boundary region of distinct composition is observed; the concentration profile looks as though it could be similar to that reported for spinodal decomposition in a confined geometry:[34] with concentrated and depleted layers. The inset to Fig. 6 shows a phase contrast image taken with a ×40 objective which seems to confirm this hypothesis. The experimental formation time observed for the water-rich layer is approximately twice that calculated assuming growth by diffusion, suggesting that molecular diffusion might not be the only effect taking place. Second, a more gradually changing structure continues to develop all the way across to the other drop (as observed macroscopically). The two different structures have been delimited by yellow lines in Fig. 6(a). A two-stage dissolution phenomenon has also been reported previously for sessile drops containing electrolyte and graphene.[35] A first stage consisted of a fast formation of a water-rich layer around the drop, followed by slow diffusion-limited behaviour. This also appears to be a reasonable explanation for our initial phase-separation effect.

3.3 Bridges: behaviour over long periods

Bridge formation was studied over 24 hours, Fig. 6(b)–(d) and the drops' composition over time obtained through Raman spectroscopy (Fig. 6(e)). Initially, the bridge grew from the pure water drop towards the mixed drop; spontaneously formed small droplets are observed in the usual way, Fig. 6(b). Slightly later than the bridge itself (minutes) and in a smaller quantity, droplets may be observed inside the mixed drop. These droplets are much more mobile than the ones in the bath, they are found across the whole drop, but predominantly close to the bridge side. After a few hours a large amount of them, behaving more statically than at earlier times, could be observed inside the mixed drop, Fig. 6(c). Even more surprisingly, after ~6 hours, a stream of small droplets is observed within the left-hand drop moving away from the interface, Fig. 6(d). This secondary effect may result from the change in composition of the pure water drop which has occurred steadily by diffusion. The initially pure water drop has gained ethanol from the bath (and a very small amount of toluene which cannot be measured due to Raman peak overlap) and will eventually begin to behave like the initially mixed drop. Both drops achieve the same composition

after ~6 hours, which is the same time at which the small stream of droplets appear in the initially pure-water drop. The secondary droplet production reduces over time, although it is still visible after 24 hours. It is possible that this effect is related to the diffusion and stranding of toluene within these mixed drops. Simultaneously, the bridge density along a line connecting the two injected drops decreases to half its apparent value (as seen by bright-field microscopy) over 24 hours. This is likely to be due to droplet ripening and coalescence leading to a decrease in the density of liquid–liquid interfaces.

4 Conclusions

We have demonstrated that a composition gradient between two injected drops, in a ternary liquid system containing nanoparticles, can create a new self-assembly process. The gradient drives the diffusion of water between the two particle-stabilized drops; the resulting change in the composition of the bath phase leads to the spontaneous formation of a large population of tiny droplets. So far, this is a description of a variant of compositional ripening. However, in the presence of silica nanoparticles, the droplets aggregate in the form an elastic ''bridge'' along the path connecting the two drops. We note, the silica nanoparticles do not appear to be adsorbed to the droplet interfaces. Ostwald ripening drives the temporal evolution of the droplet sizes within the bridge; coalescence is also seen. Careful observations, especially at later times, reveal a zoo of subsidiary phenomena. A phase separated boundary layer is found close to the pure water drop on a ~100 μm scale for standard bath compositions. The spontaneous formation of droplets is also found inside the large drops. This superficially simple and well studied system is, in fact, rich and complex.

Conflicts of interest

There are no conflicts to declare.

Acknowledgements

We are grateful to Andrew Schofield for synthesizing the fluorescent silica nanoparticles and to Elena Blanco for assistance with the rheological measurements. This work was supported by the Marie Sklodowska-Curie European Training Network COLLDENSE (H2020-MSCA-ITN-2014 Grant No. 642774).

References

1 H. Song, D. L. Chen and R. F. Ismagilov, *Angew. Chem., Int. Ed.*, 2006, **45**, 7336–7356.
2 S. Lindström and H. Andersson-Svahn, *Lab Chip*, 2010, **10**, 3363–3372.
3 Á. Marn, W. van Hoeve, P. Garca-Sánchez, L. Shui, Y. Xie, M. Fontelos, J. Eijkel, A. van den Berg and D. Lohse, *Lab Chip*, 2013, **13**, 4503–4506.
4 N. Binh-Khiem, K. Matsumoto and I. Shimoyama, *Appl. Phys. Lett.*, 2008, **93**, 124101.
5 A. Ebrahimi, P. Dak, E. Salm, S. Dash, S. V. Garimella, R. Bashir and M. A. Alam, *Lab Chip*, 2013, **13**, 4248–4256.
6 S. Lach, S. M. Yoon and B. A. Grzybowski, *Chem. Soc. Rev.*, 2016, **45**, 4766–4796.
7 B. P. Binks and R. Murakami, *Nat. Mater.*, 2006, **5**, 865–869.
8 A. Hannisdal, M.-H. Ese, P. V. Hemmingsen and J. Sjöblom, *Colloids Surf., A*, 2006, **276**, 45–58.
9 D. Vella, P. Aussillous and L. Mahadevan, *Europhys. Lett.*, 2004, **68**, 7.
10 S. Sun, M. Li, F. Dong, S. Wang, L. Tian and S. Mann, *Small*, 2016, **12**, 1920–1927.
11 M. Abkarian, A. B. Subramaniam, S.-H. Kim, R. J. Larsen, S.-M. Yang and H. A. Stone, *Phys. Rev. Lett.*, 2007, **99**, 188301.
12 P. J. Beltramo, M. Gupta, A. Alicke, I. Liascukiene, D. Z. Gunes, C. N. Baroud and J. Vermant, *Proc. Natl. Acad. Sci. U. S. A.*, 2017, **114**, 10373–10378.
13 B. P. Binks, P. D. Fletcher, B. L. Holt, O. Kuc, P. Beaussoubre and K. Wong, *Phys. Chem. Chem. Phys.*, 2010, **12**, 2219–2226.
14 P. G. Moerman, H. W. Moyses, E. B. van der Wee, D. G. Grier, A. van Blaaderen, W. K. Kegel, J. Groenewold and J. Brujic, *Phys. Rev. E*, 2017, **96**, 032607.
15 H. Stephen and T. Stephen, *Solubilities of Inorganic and Organic Compounds. Ternary and Multicomponent Systems, Part II*, Pergamon, Oxford, 1964, vol. 2.
16 M. Grauzinyte, J. Forth, K. A. Rumble and P. S. Clegg, *Angew. Chem., Int. Ed.*, 2015, **54**, 1456–1460.
17 K. A. Rumble, I. D. Stoev, D. J. French, A. Abou-Hassan and P. S. Clegg, *Langmuir*, 2017, **33**, 4235–4241.
18 J. Anderson, M. Lowell and D. Prieve, *J. Fluid Mech.*, 1982, **117**, 107–121.
19 Y. Nagasaka, S. Tanaka, T. Nehira and T. Amimoto, *Soft Matter*, 2017, **13**, 6450–6457.
20 E. Rideal and J. Davies, *Interfacial Phenomena*, Academic Press, London, 1963.
21 K. J. Ruschak and C. A. Miller, *Ind. Eng. Chem. Fundam.*, 1972, **11**, 534–540.
22 C. Solans, D. Morales and M. Homs, *Curr. Opin. Colloid Interface Sci.*, 2016, **22**, 88–93.
23 J. C. López-Montilla, P. E. Herrera-Morales, S. Pandey and D. Shah, *J. Dispersion Sci. Technol.*, 2002, **23**, 219–268.
24 S. Bochner de Araujo, M. Merola, D. Vlassopoulos and G. G. Fuller, *Langmuir*, 2017, **33**, 10501–10510.
25 S. A. Vitale and J. L. Katz, *Langmuir*, 2003, **19**, 4105–4110.
26 X. Zhang, Z. Lu, H. Tan, L. Bao, Y. He, C. Sun and D. Lohse, *Proc. Natl. Acad. Sci. U. S. A.*, 2015, **112**, 9253–9257.
27 Z. Lu, H. Xu, H. Zeng and X. Zhang, *Langmuir*, 2015, **31**, 12120–12125.
28 Z. Lu, M. H. K. Schaarsberg, X. Zhu, L. Y. Yeo, D. Lohse and X. Zhang, *Proc. Natl. Acad. Sci. U. S. A.*, 2017, **114**, 10332–10337.
29 H. Tan, C. Diddens, M. Versluis, H. Butt, D. Lohse and X. Zhang, *Soft Matter*, 2017, **13**, 2749–2759.
30 K. A. White, A. B. Schofield, P. Wormald, J. W. Tavacoli, B. P. Binks and P. S. Clegg, *J. Colloid Interface Sci.*, 2011, **359**, 126–135.

31 A. Imhof, M. Megens, J. Engelberts, D. De Lang, R. Sprik and W. Vos, *J. Phys. Chem. B*, 1999, **103**, 1408–1415.
32 J. Schindelin, I. Arganda-Carreras, E. Frise, V. Kaynig, M. Longair, T. Pietzsch, S. Preibisch, C. Rueden, S. Saalfeld and B. Schmid, *et al.*, *Nat. Methods*, 2012, **9**, 676–682.
33 F. P. Lees and P. Sarram, *J. Chem. Eng. Data*, 1971, **16**, 41–44.
34 H. Tanaka and T. Araki, *Europhys. Lett.*, 2000, **51**, 154–160.
35 Y. Song, Z. Lu, H. Yang, S. Zhang and X. Zhang, *Langmuir*, 2016, **32**, 10296–10304.